Received: 20 December 2023 | Revised: 4 March 2024 | Accepted: 25 March 2024

DOI: 10.1002/ijc.34957

RESEARCH ARTICLE

Tumor Markers and Signatures

IJC INTERNATIONAL JOURNAL of CANCER | UICC

Cancer-associated fibroblast activation predicts progression, metastasis, and prognosis of cutaneous squamous cell carcinoma

Jaakko S. Knuutila[1,2] | Pilvi Riihilä[1,2] | Liisa Nissinen[1,2] | Lauri Heiskanen[1,2] | Roosa E. Kallionpää[3] | Teijo Pellinen[4] | Veli-Matti Kähäri[1,2]

[1]Department of Dermatology, University of Turku and Turku University Hospital, Turku, Finland

[2]FICAN West Cancer Research Laboratory, University of Turku and Turku University Hospital, Turku, Finland

[3]Auria Biobank, Turku University Hospital and University of Turku, Turku, Finland

[4]Institute for Molecular Medicine Finland (FIMM), Helsinki Institute of Life Science (HiLIFE), Helsinki, Finland

Correspondence
Veli-Matti Kähäri, Department of Dermatology, University of Turku and Turku University Hospital, Hämeentie 11 TE6, FI-20520 Turku, Finland.
Email: veli-matti.kahari@utu.fi

Teijo Pellinen, Institute for Molecular Medicine Finland (FIMM), Helsinki Institute of Life Science, University of Helsinki, Tukholmankatu 8, FI-00290 Helsinki, Finland.
Email: teijo.pellinen@helsinki.fi

Funding information
Varsinais-Suomen Sairaanhoitopiiri; Suomen Lääketieteen Säätiö; Sigrid Juséliuksen Säätiö; Maud Kuistilan Muistosäätiö; Syöpäsäätiö; Jane ja Aatos Erkon Säätiö; Suomen Ihotautilääkäriyhdistys; Lounais-Suomen Syöpäyhdistys; Päivikki ja Sakari Sohlbergin Säätiö; Ida Montinin Säätiö

Abstract

Cutaneous squamous cell carcinoma (cSCC) is the most common metastatic skin cancer and the metastatic disease is associated with poor prognosis. Cancer-associated fibroblasts (CAFs) promote progression of cancer, but their role in cSCC is largely unknown. We examined the potential of CAF markers in the assessment of metastasis risk and prognosis of primary cSCC. We utilized multiplexed fluorescence immunohistochemistry for profiling CAF landscape in metastatic and non-metastatic primary human cSCCs, in metastases, and in premalignant epidermal lesions. Quantitative high-resolution image analysis was performed with two separate panels of antibodies for CAF markers and results were correlated with clinical and histopathological parameters including disease-specific mortality. Increased stromal expression of fibroblast activation protein (FAP), α-smooth muscle actin, and secreted protein acidic and rich in cysteine (SPARC) were associated with progression to invasive cSCC. Elevation of FAP and platelet-derived growth factor receptor-β (PDGFRβ) expression was associated with metastasis risk of primary cSCCs. High expression of PDGFRβ and periostin correlated with poor prognosis. Multimarker combination defined CAF subset, PDGFRα−/PDGFRβ+/FAP+, was associated with invasion and metastasis, and independently predicted poor disease-specific survival. These results identify high PDGFRβ expression alone and multimarker combination

Previously Presented Work: Part of the findings in this manuscript was previously presented in the Doctoral Thesis of Jaakko S. Knuutila. Thesis can be accessed in https://www.utupub.fi/handle/10024/173026.

PDGFRα−/PDGFRβ+/FAP+ by CAFs as potential biomarkers for risk of metastasis and poor prognosis.

KEYWORDS
epidermolysis bullosa, fibroblast, metastasis, squamous cell carcinoma

What's new?

Assessing metastatic risk and prognosis of cutaneous squamous cell carcinoma (cSCC) is hindered by a lack of biomarkers. Cancer-associated fibroblasts (CAFs), however, may yield markers relevant to prognosis, owing to their possible association with cSCC progression. Here, CAFs were investigated for associations with cSCC metastasis and prognosis using multiplexed fluorescence immunohistochemistry. The proportion of CAFs expressing platelet-derived growth factor receptor-β (PDGFRβ) was elevated in metastatic cSCC. Likewise, metastasis and poor prognosis were associated with CAF PDGFRβ positivity, PDGFRα negativity, and fibroblast activation protein (FAP) expression. The findings offer novel insight into the role of CAFs in cSCC progression and metastasis.

1 | INTRODUCTION

Cutaneous squamous cell carcinoma (cSCC) is the most common metastatic skin cancer with increasing incidence globally.[1,2] The metastasis rate of primary cSCCs has been estimated at 1%–4%, accounting for ~20% of skin cancer-related mortality.[2–4] Disease-specific mortality in cSCC is primarily associated with metastasis and prognosis of patients with metastatic disease is generally poor with 3-year overall survival (OS) of 29%–46%.[3–5] The most important risk factor for the development of cSCC is long term exposure to solar ultraviolet (UV) radiation.[6] UV-induced premalignant epidermal lesions, actinic keratoses (AK) and preinvasive in situ cSCC (cSCCIS), progress to invasive cSCC.[7] Other risk factors for cSCC include immunosuppression and chronic ulceration.[8]

Established tumor staging systems by American Joint Committee on Cancer (AJCC) and Brigham and Women's Hospital (BWH) are utilized in the clinical risk assessment of cSCC patients. Tumor diameter, invasion depth, and perineural invasion are associated with the risk of metastasis and are pivotal factors in both the BWH and the 8th edition of AJCC (AJCC-8) staging systems.[9] However, these systems are suboptimal in predicting the metastasis risk of primary cSCCs.[10] At present, no clinically established biomarkers are available for the assessment of metastasis risk or prognosis of patients with cSCC.

There is increasing evidence for the important role of tumor microenvironment (TME) in the development and progression of cancer.[11] TME consists of extracellular matrix (ECM) components and cells including cancer-associated fibroblasts (CAFs).[12] CAFs constitute a major component of TME also in cSCC, where they promote tumor initiation, progression, and metastasis.[13] CAFs are heterogeneous and plastic cells, which exert both pro- and antitumorigenic properties and the activation profile of CAFs evolves during cancer progression resulting in functional heterogeneity.[13] Several biomarkers have been used to identify and classify CAFs, but none of them are specific, suggesting that application of multiple markers could result in more accurate CAF classification.[13] These markers include α-smooth muscle actin (αSMA), fibroblast activation protein (FAP), platelet-derived growth factor receptor-α (PDGFRα), PDGFRβ, and vimentin (VIM).[12] CAFs are often classified as subtypes with ECM producing contractile phenotype (myCAFs), which typically express αSMA, and as subtypes with immunomodulating secretome (iCAFs), in addition to numerous other subtypes.[13,14] Secreted protein acidic and rich in cysteine (SPARC) or osteonectin and periostin (POSTN) are ECM proteins expressed by fibroblasts that reflect changes in tumor stroma and CAF activation during cancer progression.[15,16] Type I collagen (Col1) is a fibroblast-derived fibrillar collagen and the most abundant ECM component in skin.[17]

At present, there is limited evidence for the role of CAFs in the progression of cSCC, but three to four major fibroblast subtypes have been identified already in healthy human skin.[18,19] Here, we have evaluated the potential of CAF markers as biomarkers for progression, metastasis and prognosis in cSCC using multiplexed fluorescence immunohistochemistry (mfIHC), which enables simultaneous detection of multiple protein markers.[20] The results show, that elevated expression of FAP and PDGFRβ is associated with the risk of metastasis and high expression of PDGFRβ and POSTN correlates with poor prognosis. Furthermore, a multimarker (PDGFRα−/PDGFRβ+/FAP+) CAF subset is associated with invasion and metastasis and independently predicts poor disease-specific survival.

2 | MATERIALS AND METHODS

2.1 | Tissue RNA and NanoString expression profiling

Human primary non-metastatic ($n = 3$) and metastatic ($n = 2$) cSCC samples were obtained from surgically removed tumors in Turku University Hospital after informed consent.[21] Total RNA was isolated from the

tissue samples as previously described.[21] RNA (100 ng) was hybridized overnight at 65°C with the Human Fibrosis Panel, Cancer Progression Panel and Cancer Pathways Panel (NanoString Technologies, Seattle, WA). nCounter Prep Station was used for purification and binding of the hybridized probes to the cartridge. The scanning of the cartridge was prepared with the nCounter Digital Analyzer (NanoString Technologies). The data analysis was prepared by using nSolver 4.0 (NanoString Technologies, Seattle, WA). The quality of the data was confirmed and normalization was done by using the default QC settings.

2.2 | Tissue material

Tissue microarrays (TMAs) representing study cohorts consisting of formalin-fixed, paraffin-embedded (FFPE) human tissue specimens obtained by resection or biopsy were constructed, as previously described.[22] TMAs contain cores representing normal skin ($n = 73$), benign epidermal tumors: seborrheic keratoses (SKs) ($n = 17$), premalignant lesions: AKs ($n = 67$), cSCCISs ($n = 59$), UV-cSCCs ($n = 217$, 143 individual tumors) including non-mcSCCs ($n = 146$, 110 individual tumors) and mcSCCs, ($n = 71$, 33 individual tumors), and metastases of UV-cSCCs ($n = 16$, 11 individual metastases). In addition, recessive dystrophic epidermolysis bullosa (RDEB)-associated cSCCs (RDEBSCCs) ($n = 77$, 12 individual tumors) were included.[22] Above-mentioned numbers represent the number of TMA cores with approved high-quality mfIHC stainings. Normal skin specimens represent specimens from both sun-protected and sun-exposed skin. In analyses, mean value of the expression of all TMA cores representing each individual UV-cSCC (non-mcSCC and mcSCC), RDEBSCC and metastasis were utilized. There were 1–4 TMA cores representing each non-mcSCC, 1–9 for each mcSCC, 1–11 for each RDEBSCC, and 1–2 TMA cores for each metastasis. For premalignant and benign lesions each TMA core represents individual lesion.

Clinical and histopathological data corresponding to individual UV-cSCCs were manually obtained from patient records, as described previously.[4] All mcSCCs developed at least one nodal metastasis and part also extranodal metastases. Patients with non-mcSCCs did not develop metastases during at least 5-year follow-up.[4] The 5-year cSCC-specific survival of patients with UV-induced non-mcSCC or mcSCC was deduced from the patient records and calculated from the date of initial diagnosis of the primary UV-cSCC. Baseline characteristics of UV-induced non-mcSCCs and mcSCCs, validation cohort mcSCCs and RDEBSCCs are shown in Table S1.

2.3 | Validation cohort

For validation purposes another cohort of UV-induced primary mcSCCs was created of our tumor material characterized previously.[4] This cohort comprised of 37 TMA cores representing 18 additional individual primary mcSCCs, which were stained and analyzed with panel 1 and compared to the cohort of UV-induced non-mcSCCs described above.

2.4 | RDEBSCC dataset

RDEBSCC gene expression profile dataset GSE111582[23] was downloaded from the publicly available Gene Expression Omnibus (GEO) and utilized to analyze the expression of CAF markers in RDEBSCC samples ($n = 8$) investigated in our study.

2.5 | Multiplexed fluorescence immunohistochemistry and panels

CAF markers and their distribution in stromal and epithelial compartments were defined using two mfIHC panels containing PDGFRβ, PDGFRα, αSMA, and FAP in panel 1, and SPARC, PDGFRβ, POSTN, Col1, and VIM in panel 2 (Table S2). PanEpi cocktail was used to detect epithelial cells (Table S2). The mRNAs for these markers are expressed in tumor tissue of UV-induced cSCCs and RDEBSCCs (Figure S1, Tables S3–S5).

2.6 | Imaging and image analysis

The whole-slide TMA imaging (to achieve 5-channel fluorescence images) was implemented using Axio Scan.Z1 Digital Slide Scanner (The Zeiss™, Germany) equipped with ×20 (0.8NA) Plan-Apochromat objective (The Zeiss™, Germany), ORCA-Flash 4.0 V2 Digital CMOS camera (Hamamatsu Photonics K.K., Japan) and Colibri.7 LED light source (The Zeiss™, Germany). DAPI, FITC, Cy3, Cy5, and Cy7 filters were used.

Following the whole-slide TMA imaging, the 5-channel fluorescence images were exported as single-channel grayscale images (64 Bit, Big Tiff Format) and resized to a quarter of the original image size. The images were cropped to individual TMA cores using ImageJ (version 1.53M for Windows) with Roi1 1-Click Tools. The TMA core images from the second staining round were registered (overlaid) with the first-round images using nuclei (DAPI) as the reference. Registering was performed using MATLAB and Statistics Toolbox Release 2020b (The MathWorks Inc., Natick, MA). Ilastik (version 1.3.3post1 for Windows)[24] was used to detect autofluorescence (e.g., red blood cells and empty areas (background)) from the images, generating final tissue mask.

The final image analysis pipeline was performed using CellProfiler (version 4.2.1).[25] Tasked tissue was classified into epithelium and stromal compartments by thresholding the epithelial channel (epithelial compartment) and subtracting the epithelium from the total final tissue (stroma compartment). Each marker was set as negative or positive for every single pixel by careful visual determination of the positivity threshold. Different marker combinations were defined by using "mask image" module. The total number of marker classified pixels was measured in both the epithelial and stromal compartments. Fractions of positive marker and marker combinations were counted by dividing them with total either epithelial or stromal pixels, generating results for relative cell areas. Mean intensities of channels were also measured in the different compartments.

Expression level of every marker in both panels was analyzed independently in both stromal and epithelial compartments for both the relative cell area and intensity (Table S6). Furthermore for panel 1, 18 CAF subsets based on combination of two markers (CAFa-r), 28 CAF subsets based on combination of three markers (CAF101-128) and 15 CAF subsets based on combination of four markers (CAF1-15) were generated (Table S6). For panel 2 additional nine CAF subsets based on combination of two markers (CAF1a-1i) were created (Table S6). Multimarker subsets were analyzed only for stromal compartment.

2.7 | Statistical analysis

Two different analysis paths were followed: one for all different tissue types (normal skin, SKs, AKs, cSCCISs, UV-cSCCs, metastases, and RDEBSCCs) and another for UV-induced non-mcSCCs and mcSCCs. All statistical analyses were conducted using IBM SPSS Statistics for Windows, version 25.0 (IBM Corp., Armonk, NY) and/or R statistical Software 4.1.1 (Foundation for Statistical Computing, Vienna, Austria). Statistical significance was based on the 95% confidence level and all the tests were two-tailed. Independent samples Kruskal–Wallis *H*-test with Dunn–Bonferroni post hoc method was used to test differences of ordinal and continuous variables between the seven tissue cohorts. Mann–Whitney *U* test was used in comparison of non-metastatic and metastatic UV-cSCC tumor cohorts. Binary logistic regression analyses were performed in order to determine crude ORs (cORs) with 95% CIs for the risk of metastasis. The Kaplan–Meier method with Log-Rank (Mantel–Cox) test was applied to generate survival curves and define survival estimates. Proportional hazards assumption was tested and univariate and multivariate Cox regression analyses were conducted to further visualize the prognostic influences with test for PH assumption. Statistically significant clinical binary variables in univariate Cox regression analysis were included into multivariate analysis except invasion beyond fat and staging systems (AJCC-8, BWH), which were excluded due to multicollinearity. Individual marker or marker combination was included one at a time to the model. Median, quartile, and highest quartile versus rest distributions were tested in the Kaplan–Meier and Cox regression analyses but without exception highest quartile versus rest approach resulted in best results. The reported Kaplan–Meier survivals and hazard ratios (HRs) are based on stratification between the highest quartile of values (denoted below as high and +) versus the lowest three quartiles (denoted below as low and −) with respect to markers and marker combinations. In logistic regression analyses the numerical marker values were multiplied by 100 to represent the percentage of marker or marker combination positive cells within named compartment and to make ORs more relevant.

2.8 | Bioinformatics analysis

The online Gene Expression Profiling Interactive Analysis (GEPIA; http://gepia.cancer-pku.cn/) survival analysis tool was utilized to analyze the relationship between *PDGFRB*, *FAP*, and *PDGFRA* mRNA expression and prognosis of head and neck SCC (HNSCC) and lung SCC (LUSCC) in The Cancer Genome Atlas (TCGA) data.[26,27]

3 | RESULTS

3.1 | Expression of FAP, αSMA, and SPARC is associated with invasion of cSCC

The expression of CAF markers in vivo was examined by mfIHC in TMAs containing tissue samples representing different stages of progression of UV-induced cSCC, that is, AKs ($n = 67$), cSCCISs ($n = 59$), sporadic UV-cSCCs ($n = 143$), and metastases of UV-cSCCs ($n = 11$). In comparison, the expression of CAF markers was also analyzed in tissue samples from RDEBSCCs ($n = 12$), normal skin ($n = 73$), and SK ($n = 17$). Representative images of the mfIHC stained CAF markers and their relative frequency distributions in different tissue sample types are shown in Figures 1 and 2A. Heterogeneity in the expression of CAF markers within individual tissue samples was evident (Figure 1). The cells with strong PDGFRβ, FAP, and POSTN expression were more abundant in the stroma adjacent to invasive tumor cell islets than in stroma adjacent to normal skin (Figure 1).

Stromal cells positive for FAP, αSMA, and SPARC were more prevalent in invasive primary UV-cSCCs than in AKs or cSCCISs, indicating that these markers are associated with invasion of cSCC (Figure 2A,B). In addition, proportion of stromal cells positive for POSTN was higher in UV-cSCCs than in cSCCISs (Figure 2B). In comparison, proportion of PDGFRβ positive stromal cells was similar in AKs, cSCCISs, and UV-cSCCs, whereas stromal PDGFRα positivity was more prevalent in normal skin than in UV-cSCCs (Figure 2B). Comparisons of cohorts for stromal marker expression are shown in Table S7.

Prominent stromal expression of CAF markers was noted in metastases at the same level as in UV-cSCCs except POSTN, which was more frequently noted in metastases than in primary UV-cSCCs, and VIM, which was less prevalent in metastases than in UV-cSCCs (Figure 2B).

In general, the expression of CAF markers was lower in the epithelial compartments of the tumors than in stromal tissue (Figure S2, Table S8). Mean percentages of marker and marker combination positive cells for each tissue cohort are shown in Table S8. FAP, αSMA, and PDGFRβ positive epithelial cells were more prevalent in invasive UV-cSCCs than in AKs or cSCCISs and SPARC and POSTN positive epithelial cells more prevalent in UV-cSCCs than in cSCCISs (Figure S2, Table S8). POSTN positive epithelial cells were more abundant in metastases than in UV-cSCCs and PDGFRα positive cells more prevalent in normal skin than in UV-cSCCs.

In comparison, tissue samples of cSCCs from patients with RDEB were examined. RDEBSCC is an aggressive form of cSCC, which develops in chronic ulcers of RDEB patients, and its mutation profile differs from UV-cSCC.[23,28] Our results show prominent stromal staining for FAP, αSMA, SPARC, POSTN, and VIM in RDEBSCCs (Figure 2A,B). Interestingly, the abundance of PDGFRβ and Col1 positive stromal cells was significantly lower in RDEBSCCs than in primary UV-cSCCs indicating the presence of a distinct CAF subset in this type of cSCC (Figure 2B).

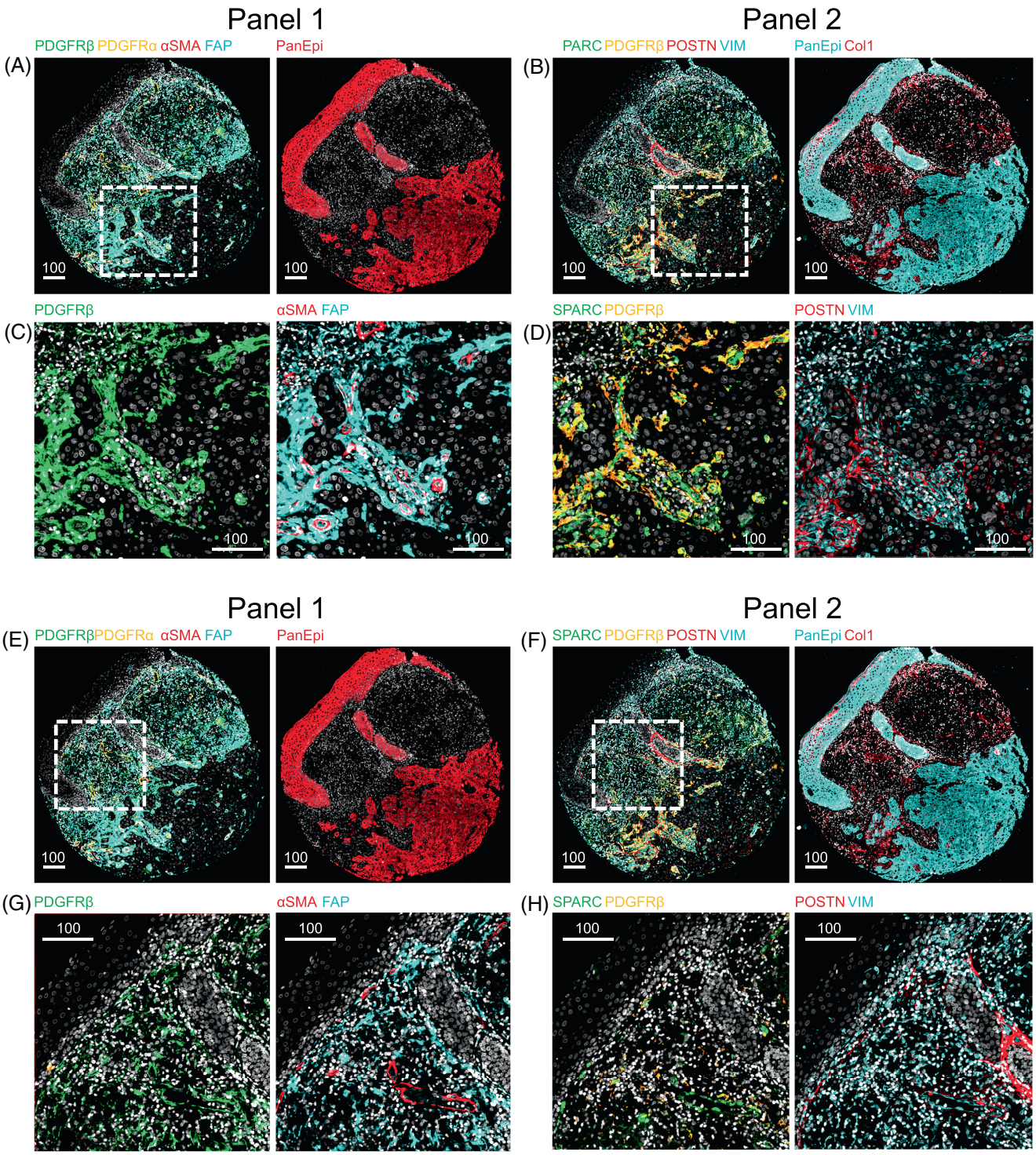

FIGURE 1 Representative multiplexed fluorescence immunohistochemistry (mfIHC) stainings of UV-induced cSCC for CAF markers. (A,B) and (E,F) mfIHC stainings of UV-cSCC tissue microarray cores with panel 1 (A,E) and panel 2 (B,F) antibodies for CAF markers. Scale bar = 100 μm. (C,D) and (G,H) High power magnifications show more prevalent stromal PDGFRβ, FAP, and POSTN expression adjacent to invasive tumor cell islets (C,D) than in the proximity of normal skin (G,H). Scale bar = 100 μm.

3.2 | Expression of PDGFRβ and FAP is associated with metastasis risk of cSCC

To elucidate the feasibility of CAF markers in the assessment of metastasis risk of cSCC, invasive UV-induced primary non-mcSCCs ($n = 110$) and mcSCCs ($n = 33$) were compared at tumor level. Representative mfIHC images demonstrate the proportion and distribution of CAF marker positive cells in non-mcSCCs and mcSCCs (Figure 3A). Stromal cells positive for PDGFRβ were more commonly detected in mcSCCs than in non-mcSCCs examined with both panel

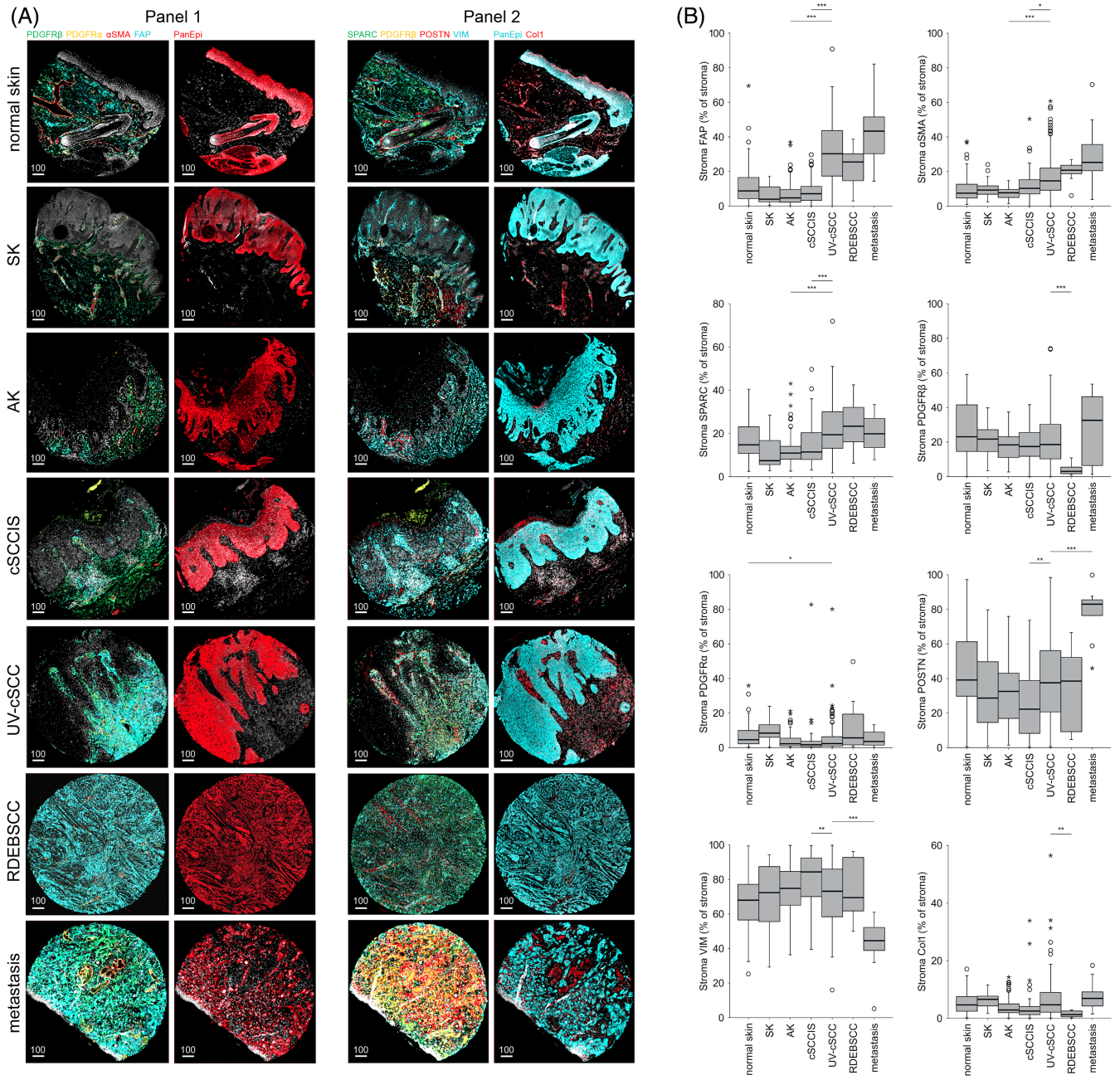

FIGURE 2 Stromal expression of CAF markers in cSCC. (A) Representative images of mfIHC stainings of normal skin, seborrheic keratosis (SK), actinic keratosis (AK), in situ cutaneous squamous cell carcinoma (cSCCIS), ultraviolet-induced invasive cutaneous squamous cell carcinoma (UV-cSCC), recessive dystrophic epidermolysis bullosa-associated cutaneous squamous cell carcinoma (RDEBSCC), and metastasis of UV-cSCC for CAF markers. Scale bar = 100 µm. (B) quantitation of the prevalence of CAF marker positive cells in stromal compartment of specimens representing above mentioned cohorts. FAP, αSMA, and SPARC positive stromal cells are more prevalent in invasive UV-cSCCs ($n = 143$) than in premalignant lesions AKs ($n = 67$) or cSCCISs ($n = 59$). Stromal PDGFRβ and Col1 expression is less frequent in RDEBSCCs ($n = 12$) than in UV-cSCCs. POSTN positive stromal cells are more abundant in UV-cSCCs than cSCCISs and in metastases ($n = 11$) than UV-cSCCs. In contrast, VIM positive stromal cells are more abundant in cSCCISs than UV-cSCCs and in UV-cSCCs than metastases. PDGFRα positive stromal cells are more frequently detected in normal skin ($n = 73$) than in UV-cSCCs. *: $P < .05$, **: $P < .01$, ***: $P < .001$ with Dunn–Bonferroni post hoc test. Clinically relevant statistical significances are shown. All statistical significances are shown in Table S7.

1 ($P = .004$) and panel 2 ($P = .006$) (Figures 3B and S3C). Similarly, stromal cells positive for FAP were more prevalent in mcSCCs than in non-mcSCCs ($P = .026$) (Figure 3B). In contrast, comparison of the two patient subgroups with respect to stromal PDGFRα, αSMA, SPARC, POSTN, VIM, or Col1 revealed no statistically significant differences (Figure S3A). In epithelial compartments, PDGFRβ and FAP positive cells were more abundant in mcSCCs than in non-mcSCC (Figure S3B,D). Additionally, cells positive for POSTN were

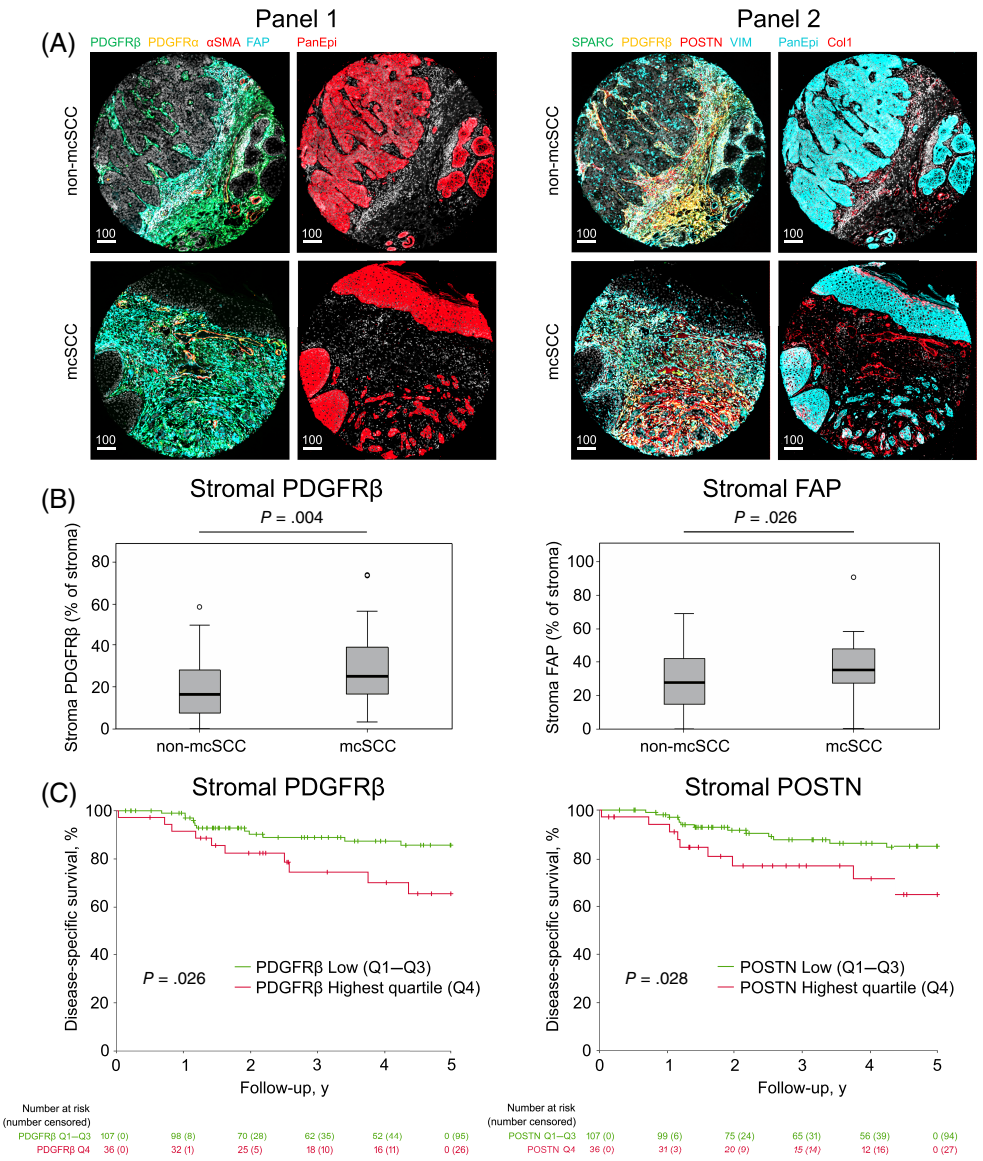

FIGURE 3 Stromal expression of CAF markers in metastatic and non-metastatic UV-induced cSCC. (A) representative images of mfIHC stainings of non-metastatic primary cSCCs (non-mcSCCs) and metastatic primary cSCC (mcSCCs). Scale bar = 100 μm. (B) PDGFRβ and FAP positive stromal cells are more prevalent in mcSCCs ($n = 33$) than in non-mcSCCs ($n = 110$). *P*-values calculated with Mann–Whitney *U* test. (C) High prevalence of PDGFRβ and POSTN positive stromal cells is associated with worse disease-specific survival in cSCC visualized by Kaplan–Meier survival estimate curves. *P*-values calculated with log-rank (Mantel–Cox) test.

more prevalent in the epithelial compartments of mcSCCs compared to non-mcSCCs (Figure S3B).

Binary logistic regression analysis was carried out to compare the value of distinct CAF markers to clinicohistopathological parameters in predicting the metastasis risk of primary cSCCs (Tables 1 and S9). The results validated with both mfIHC panels supported the observation, that higher prevalence of stromal fibroblasts positive for PDGFRβ is associated with increased metastasis risk of primary cSCCs (Table 1). In addition, elevated FAP in the stromal and epithelial compartments was associated with elevated risk of metastasis, while POSTN in the epithelial compartment only was associated with metastasis risk (Table 1).

Positive correlation between FAP, stromal PDGFRβ, epithelial POSTN, and Clark's level was noted (Table S10). On the other hand, statistically significant negative correlation between stromal PDGFRα expression and tumor diameter, invasion beyond fat and more advanced BWH tumor stage was noted (Table S10).

3.3 | PDGFRβ and POSTN expression in cSCC is associated with poor prognosis

The prognostic power of CAF markers and clinicohistopathological parameters was evaluated with Cox regression analysis and Kaplan–Meier survival estimates for patients with primary UV-cSCCs (non-mcSCCs and mcSCCs) at tumor level. High frequencies of either PDGFRβ positive or POSTN positive stromal cells correlated with worse prognosis in univariate Cox regression analysis (Tables 2 and S11). Accordingly, the prognosis of patients with primary UV-cSCC with high stromal PDGFRβ or POSTN expression was worse as determined with log-rank (Mantel–Cox) test (Figures 3C and S4A–C). While the expression of PDGFRβ in the stromal compartment was associated with worse prognosis, POSTN expression in both epithelial and stromal compartments was associated with worse prognosis (Table 2).

TABLE 1 Logistic regression analysis of CAF markers and marker combinations in association with the risk of metastasis.

Markers (continuous)	Risk of metastasis by variable cOR (95% CI)	*P* value
Panel 1 Area		
Stroma	1.02 (1.00–1.05)	.098
Epi	1.01 (0.99–1-02)	.521
PDGFRβ+ Stroma	1.04 (1.01–1.07)	.003
PDGFRβ+ Epi	1.05 (0.95–1.16)	.333
PDGFRα+ Stroma	0.95 (0.87–1.03)	.216
PDGFRα+ Epi	0.95 (0.85–1.07)	.391
FAP+ Stroma	1.03 (1.00–1.05)	.029
FAP+ Epi	1.03 (1.00–1.06)	.036
αSMA+ Stroma	1.01 (0.98–1.05)	.359
αSMA+ Epi	0.97 (0.87–1.07)	.493
PDGFRβ+/FAP+ Stroma (CAFd)	1.06 (1.02–1.10)	.002
PDGFRβ+/αSMA+ Stroma (CAFf)	1.07 (1.01–1.12)	.012
PDGFRβ+/PDGFRα− Stroma (CAFk)	1.05 (1.02–1.08)	.001
PDGFRβ+/αSMA− Stroma (CAFl)	1.05 (1.01–1.09)	.014
FAP+/PDGFRα− Stroma (CAFr)	1.03 (1.00–1.05)	.028
PDGFRβ+/FAP+/αSMA+ Stroma (CAF101)	1.07 (1.00–1.14)	.042
PDGFRα−/PDGFRβ+/αSMA+ Stroma (CAF103)	1.08 (1.02–1.14)	.007
PDGFRα−/FAP+/PDGFRβ+ Stroma (CAF107)	1.07 (1.03–1.11)	.001
PDGFRβ+/FAP+/αSMA− Stroma (CAF113)	1.09 (1.03–1.14)	.002
PDGFRβ+/PDGFRα−/αSMA− Stroma (CAF127)	1.06 (1.02–1.10)	.006
PDGFRβ+/FAP+/PDGFRα−/αSMA− Stroma (CAF6)	1.10 (1.04–1.17)	.001
PDGFRβ+/FAP+/PDGFRα−/αSMA+ Stroma (CAF7)	1.08 (1.01–1.16)	.035
Panel 2 Area		
StromaImage	1.03 (1.00–1.06)	.056
PanEpiImage	1.00 (0.98–1.02)	.973
SPARC+ Stroma	1.00 (0.97–1.04)	.848
SPARC+ Epi	1.04 (0.99–1.09)	.091
PDGFRβ+ Stroma	1.07 (1.01–1.12)	.013
PDGFRβ+ Epi	1.31 (0.87–1.98)	.201
POSTN+ Stroma	1.01 (1.00–1.03)	.137
POSTN+ Epi	1.05 (1.00–1.09)	.044
VIM+ Stroma	0.99 (0.97–1.02)	.561
VIM+ Epi	1.05 (1.00–1.10)	.056
Col1+ Stroma	0.99 (0.93–1.05)	.710
Col1+ Epi	0.97 (0.91–1.04)	.424
PDGFRβ+/POSTN+ Stroma	1.14 (1.04–1.26)	.006
PDGFRβ+/SPARC+ Stroma	1.13 (1.03–1.24)	.013
VIM+/PDGFRβ+ Stroma	1.09 (1.02–1.16)	.014
VIM+/POSTN+ Stroma	1.04 (1.00–1.08)	.038

Note: Cancer-associated fibroblast (CAF) markers and CAF subsets, that is, marker combinations with statistically significant association with the risk of metastasis are shown. For CAF markers and CAF subsets the variables are treated as continuous. cSCC (mcSCCs) ($n = 33$) and non-metastatic cSCCs (non-mcSCCs) ($n = 110$) were compared.

Abbreviations: CI, confidence interval; Col1, type I collagen; cOR, crude odds ratio; FAP, fibroblast activation protein; PDGFRα, platelet-derived growth factor receptor-α; PDGFRβ, platelet-derived growth factor receptor-β; POSTN, periostin; SPARC, secreted protein acidic and rich in cysteine; VIM, vimentin; αSMA, α-smooth muscle actin.

TABLE 2 Univariate and multivariate Cox regression analysis of clinical and histopathological variables, CAF markers, and marker combinations in association with prognosis of patients with cSCC.

Variable	Non-mcSCC pos/total	mcSCC pos/total	Univariate Cox cHR (95% CI)	*P* value	Multivariate Cox aHR (95% CI)	*P* value	Multivariate Cox aHR (95% CI)	*P* value
Age								
1st–3rd quartile (27–84 years), *n* (%)	80/110 (72.7)	27/33 (81.8)	0.83 (0.28–2.47)	.736				
4th quartile (85–102 years), *n* (%)	30/110 (27.3)	6/33 (18.2)	1 (ref)					
Gender								
Male, *n* (%)	69/110	23/33	0.79 (0.37–1.84)	.581				
Female, *n* (%)	41/110	13/33	1 (ref)					
Location								
Head and neck, *n* (%)	92/110 (83.6)	24/33 (72.7)	1 (ref)	.299				
Other, *n* (%)	8/110 (7.3)	4/33 (12.1)	1.65 (0.64–4.21)					
Missing, *n* (%)	1/110 (0.9)	0/33 (0.0)						
Diameter								
<30 mm, *n* (%)	91/110 (82.7)	11/33 (33.3)	1 (ref)		1 (ref)		1 (ref)	
≥30 mm, *n* (%)	19/110 (17.3)	22/33 (66.7)	12.49 (4.57–34.13)	<.001	5.52 (1.56–19.52)	.008	4.83 (1.47–15.83)	.009
Differentiation								
Good or moderate, *n* (%)	98/110 (89.1)	25/33 (75.8)	1 (ref)		1 (ref)		1 (ref)	
Poor, *n* (%)	12/110 (10.9)	8/33 (24.2)	3.21 (1.25–8.24)	.016	1.89 (0.64–5.57)	.248	2.06 (0.69–6.16)	.197
Necrosis among primary tumor								
No, *n* (%)	101/110 (91.8)	26/33 (78.8)	1 (ref)		1 (ref)		1 (ref)	
Yes, *n* (%)	7/110 (6.4)	6/33 (18.2)	3.87 (1.42–10.57)	.008	1.15 (0.39–3.46)	.798	1.20 (0.41–3.56)	.740
Missing, *n* (%)	2/110 (1.8)	1/33 (3.0)						
Clark's level								
2–4, *n* (%)	78/110 (70.9)	5/33 (15.2)	1 (ref)		1 (ref)		1 (ref)	
5, *n* (%)	30/110 (27.3)	27/33 (81.8)	10.79 (3.17–36.68)	<.001	2.34 (0.48–11.42)	.295	2.59 (0.60–11.25)	.205
Missing, *n* (%)	2/110 (1.8)	1/33 (3.0)						
Invasion beyond fat								
No, *n* (%)	96/110 (87.3)	16/33 (48.5)	1 (ref)					
Yes, *n* (%)	14/110 (12.7)	16/33 (48.5)	5.20 (2.21–12.26)	<.001				
Missing, *n* (%)	0/110 (0.0)	1/33 (3.0)						
Diffuse growth pattern								
No, *n* (%)	104/110 (94.5)	28/33 (84.8)	1 (ref)		1 (ref)		1 (ref)	
Yes, *n* (%)	5/110 (4.5)	5/33 (15.2)	5.26 (1.93–14.36)	.001	1.75 (0.55–5.55)	.342	1.80 (0.57–5.73)	.318
Missing, *n* (%)	1/110 (0.9)	0/33 (0.0)						

(Continues)

TABLE 2 (Continued)

Variable	Non-mcSCC pos/total	mcSCC pos/total	Univariate Cox cHR (95% CI)	*P* value	Multivariate Cox aHR (95% CI)	*P* value	Multivariate Cox aHR (95% CI)	*P* value
AJCC-8								
T1-T3, *n* (%)	107/110 (97.3)	27/33 (81.8)	1 (ref)					
T4a-T4b, *n* (%)	3/110 (2.7)	5/33 (15.2)	4.28 (1.44–12.74)	.009				
TX, *n* (%)	0/110 (0.0)	1/33 (3.0)						
BWH								
T1-T2b, *n* (%)	72/110 (65.5)	5/33 (15.2)	1 (ref)					
T3, *n* (%)	3/110 (2.7)	5/33 (15.2)	5.69 (2.08–15.55)	.001				
TX, *n* (%)	0/110 (0.0)	1/33 (3.0)						
Markers (highest quartile)								
Panel 1 Area								
Stroma, *n* (%)	27/110 (24.5)	9/33 (27.3)	1.08 (0.42–2.77)	.869				
Epi, *n* (%)	27/110 (24.5)	9/33 (27.3)	1.55 (0.63–3.81)	.338				
PDGFRβ+ Stroma, *n* (%)	25/110 (22.7)	11/33 (33.3)	2.51 (1.08–5.81)	.032				
PDGFRβ+ Epi, *n* (%)	25/110 (22.7)	11/33 (33.3)	1.96 (0.84–4.59)	.121				
PDGFRα+ Stroma, *n* (%)	31/110 (28.2)	5/33 (15.2)	0.45 (0.13–1.53)	.202				
PDGFRα+ Epi, *n* (%)	29/110 (26.4)	7/33 (21.2)	0.62 (0.21–1.84)	.392				
FAP+ Stroma, *n* (%)	25/110 (22.7)	11/33 (33.3)	1.93 (0.81–4.59)	.140				
FAP+ Epi, *n* (%)	24/110 (21.8)	12/33 (36.4)	1.83 (0.77–4.37)	.172				
αSMA+ Stroma, *n* (%)	27/110 (24.5)	9/33 (27.3)	1.44 (0.59–3.53)	.426				
αSMA+ Epi, *n* (%)	29/110 (26.4)	7/33 (21.2)	0.78 (0.29–2.12)	.631				
PDGFRβ+/**FAP**+ Stroma (**CAFd**), *n* (%)	21/110 (19.1)	15/33 (45.5)	2.94 (1.27–6.78)	.012				
PDGFRβ+/**PDGFRα**− Stroma (**CAFk**), *n* (%)	24/110 (21.8)	12/33 (36.4)	3.14 (1.36–7.26)	.007				
FAP+/**PDGFRα**− Stroma (**CAFr**), *n* (%)	24/110 (21.8)	12/33 (36.4)	2.41 (1.03–5.63)	.043				
PDGFRα−/**FAP**+/**PDGFRβ**+ Stroma (**CAF107**), *n* (%)	21/110 (19.1)	15/33 (45.5)	3.99 (1.72–9.24)	.001	2.74 (1.10–6.81)	.030		
PDGFRβ+/**FAP**+/**αSMA**− Stroma (**CAF113**), *n* (%)	21/110 (19.1)	15/33 (45.5)	3.21 (1.39–7.40)	.006				
PDGFRβ+/**PDGFRα**−/**αSMA**− Stroma (**CAF127**), *n* (%)	23/110 (20.9)	13/33 (39.4)	3.85 (1.66–8.92)	.002				
PDGFRβ+/FAP+/PDGFRα−/αSMA− Stroma (CAF6), *n* (%)	20/110 (18.2)	16/33 (48.5)	4.95 (2.11–11.62)	<.001			3.31 (1.33–8.25)	.010
Panel 2 Area								
StromaImage, *n* (%)	25/110 (22.7)	11/33 (33.3)	1.60 (0.65–3.94)	.303				
PanEpiImage, *n* (%)	28/110 (25.5)	8/33 (24.2)	1.56 (0.64–3.84)	.329				

TABLE 2 (Continued)

Variable	Non-mcSCC pos/total	mcSCC pos/total	Univariate Cox cHR (95% CI)	*P* value	Multivariate Cox aHR (95% CI)	*P* value	Multivariate Cox aHR (95% CI)	*P* value
SPARC+ Stroma, *n* (%)	28/110 (25.5)	8/33 (24.2)	0.59 (0.20–1.74)	.335				
SPARC+ Epi, *n* (%)	25/110 (22.7)	11/33 (33.3)	1.55 (0.63–3.80)	.341				
PDGFRβ+ Stroma, *n* (%)	24/110 (21.8)	12/33 (36.4)	2.32 (0.99–5.44)	.052				
PDGFRβ+ Epi, *n* (%)	22/110 (20.0)	14/33 (42.4)	2.10 (0.90–4.91)	.087				
POSTN+ Stroma, *n* (%)	25/110 (22.7)	11/33 (33.3)	2.52 (1.08–5.91)	.034				
POSTN+ Epi, *n* (%)	24/110 (21.8)	12/33 (36.4)	3.18 (1.37–7.41)	.007				
VIM+ Stroma, *n* (%)	31/110 (28.2)	5/33 (15.2)	0.48 (0.14–1.62)	.238				
VIM+ Epi, *n* (%)	25/110 (22.7)	11/33 (33.3)	1.41 (0.57–3.45)	.457				
Col1+ Stroma, *n* (%)	29/110 (26.4)	7/33 (21.2)	1.34 (0.55–3.28)	.526				
Col1+ Epi, *n* (%)	29/110 (26.4)	7/33 (21.2)	0.77 (0.28–2.08)	.604				
PDGFRβ+/**Postn**+ Stroma, *n* (%)	21/110 (19.1)	15/33 (45.5)	3.93 (1.70–9.11)	.001				
VIM+/**PDGFRβ**+ Stroma, *n* (%)	22/110 (20.0)	14/33 (42.4)	2.71 (1.17–6.27)	.020				

Note: Cancer associated fibroblast (CAF) subsets i.e. marker combinations with statistically significant associations are shown. Multivariate analyses are visualized both with CAF107 and CAF6 subset. For CAF markers and CAF subsets highest quartile represents positivity. Only proportions of marker positive cells are shown.

Abbreviations: aHR, adjusted hazard ratio; AJCC-8, 8th edition of American Joint Committee on Cancer tumor staging; BWH, Brigham and Women's Hospital tumor staging; cHR, crude hazard ratio; CI, confidence interval; Col1, type I collagen; FAP, fibroblast activation protein; PDGFRα, platelet-derived growth factor receptor-α; PDGFRβ, platelet-derived growth factor receptor-β; pos, positive; POSTN, periostin; SPARC, secreted protein acidic and rich in cysteine; VIM, vimentin; αSMA, α-smooth muscle actin.

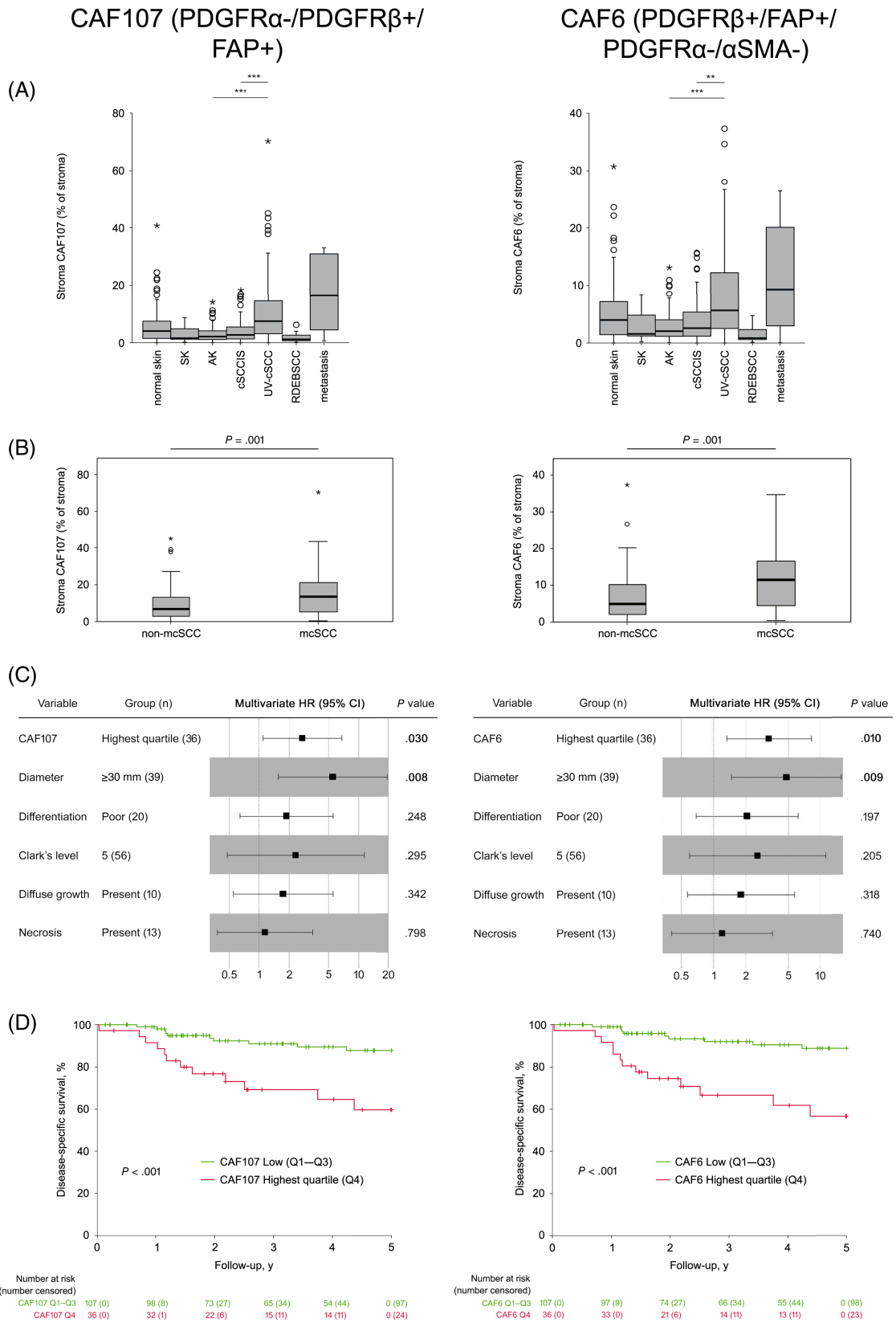

FIGURE 4 Legend on next page.

3.4 | Multimarker combination PDGFRα−/PDGFRβ+/FAP+ is associated with invasion, metastasis, and poor prognosis of cSCC

Multimarker combinations associated with distinct CAF subsets (Table S6) were analyzed with respect to invasion and metastasis of tumors and prognosis of the patients. Several CAF subsets were associated with invasive cSCCs, including CAF107 (PDGFRα−/PDGFRβ+/FAP+) and CAF6 (PDGFRβ+/FAP+/PDGFRα−/αSMA−) (Figure 4A and Table S7). Furthermore, 16 CAF subsets were found to be associated with increased metastasis risk (Table 1). The subsets with most significant p values include CAF107 and CAF6 (Table 1 and Figure 4B). Nine CAF subsets including CAF107 and CAF6 were found to be associated with poor prognosis using univariate Cox regression analysis (Table 2). Each CAF subset with statistically significant association in univariate analysis was also analyzed separately in multivariate setting adjusted for clinical variables associated with risk of metastasis. Only CAF107 and CAF6 subsets were associated with worse prognosis with statistically significant adjusted HRs (Table 2 and Figure 4C). The association between these CAF subsets and poor prognosis is shown in Kaplan–Meier survival estimate curves (Figure 4D).

CAF107 phenotype positively correlated with diameter, poor differentiation and high Clark's level of the primary tumor (Table S10). CAF6 subset positively correlated with poorer differentiation and higher Clark's level and negatively with high age (Table S10).

3.5 | Validation of CAF markers

For validation purposes another cohort comprising of UV-induced primary mcSCCs ($n = 18$) was compared to UV-induced non-mcSCCs ($n = 110$). The results confirmed the findings above on the association between metastasis risk and stromal PDGFRβ and FAP expression (Figure S5A and Table S12). Additionally, the association between metastasis risk and CAF107 subset was confirmed (Figure S5B and Table S12).

For additional validation of the individual CAF markers, we analyzed gene expression data from TCGA to determine, whether PDGFRα, PDGFRβ, and FAP, included in CAF107 subset, have prognostic value in other SCCs. High expression of PDGFRβ was associated with poor prognosis in lung SCC (Figure S4D). Furthermore, analysis of HNSCC cohort in the TCGA data showed, that high expression of FAP was associated with worse prognosis and expression of PDGFRα was associated with better prognosis (Figure S4D).

4 | DISCUSSION

In the present study, we have analyzed a large panel of human cSCC tissue specimens with mfIHC to elucidate whether changes in the expression of individual CAF markers or specific marker combinations are associated with the metastasis risk of cSCC. Our results show, that elevated expression of FAP, αSMA, and SPARC in stromal fibroblasts is associated with the development of invasive UV-cSCC. In addition, we observed that the proportion of PDGFRβ positive CAFs is higher in mcSCCs than in non-mcSCCs. Furthermore, analysis of different CAF subsets revealed, that PDGFRβ positivity in multimarker combinations (CAF107, CAF6) was also associated with metastasis and poor prognosis, indicating the pivotal role of PDGFRβ in metastasis of cSCC.

Previously, four fibroblast subtypes with distinct expression profiles have been identified in healthy skin: pro-inflammatory, secretory–papillary, secretory–reticular, and mesenchymal.[18,29] These subpopulations can be observed during the entire cSCC disease continuum but their proportions change during tumor progression.[29] It has been shown, that CAFs are absent in premalignant AK and that iCAF predominance changes to myCAF predominance, as cSCCIS progresses to invasive cSCCs.[29] In addition, FAP and αSMA expression increases in cSCCIS and cSCC.[29]

Previous studies have demonstrated that stromal fibroblasts expressing PDGFRs promote cancer metastasis in response to paracrine stimulation by PDGF produced by adjacent tumor cells.[30–32] In addition to CAFs, PDGFRβ is expressed by perivascular cells.[33] In colon cancer, CAFs derived from mesenchymal stem cells express high levels of PDGFRβ, which is associated with vascularization and metastatic potential.[31,32] Furthermore, expression of PDGFRβ in stromal fibroblasts is associated with worse prognosis in breast and prostate cancers and correlates with clinical and histopathological markers associated with poor prognosis.[34–36] These results are in accordance with previous observations showing high expression of PDGFRβ in cSCC.[37]

The role of PDGFRα in cancer is less well known. Our observations show, that PDGFRα expression is higher in normal skin than in UV-cSCCs, suggesting a tumor suppressive function. In normal human skin, the expression of PDGFRα is high in fibroblasts in papillary dermis, whereas the expression in fibroblasts in reticular dermis is

FIGURE 4 CAF subsets CAF107 (PDGFRα−/PDGFRβ+/FAP+) and CAF6 (PDGFRβ+/FAP+/PDGFRα−/αSMA−) are associated with invasion, metastasis and poor prognosis of cutaneous squamous cell carcinoma (cSCC). (A) Both CAF107 and CAF6 subsets are more frequent in ultraviolet-induced invasive cSCCs (UV-cSCCs) ($n = 143$) than in actinic keratoses (AKs) ($n = 67$) or in situ cutaneous squamous cell carcinomas (cSCCISs) ($n = 59$). Normal skin ($n = 73$), SK ($n = 17$) RDEBSCCs ($n = 12$), metastasis ($n = 11$). **: $P < .01$, ***: $P < .001$ with Dunn–Bonferroni post hoc test. (B) CAF107 and CAF6 subsets are more frequent in metastatic cSCCs (mcSCCs) ($n = 33$) than in non-metastatic cSCCs (non-mcSCCs) ($n = 110$). (C) Multivariate Cox regression analysis shows, that high prevalence of CAF107 and CAF6 subsets is independently associated with worse prognosis with primary tumor diameter. (D) Kaplan–Meier survival estimate curves show, that high prevalence of CAF107 and CAF6 subsets in primary cSCC is associated with worse disease-specific survival. *P*-values calculated with log-rank (Mantel–Cox) test.

lower.[38] It has been shown that fewer pro-inflammatory and secretory–reticular fibroblasts are detected in cSCC tumors but the number of mesenchymal fibroblasts is significantly increased compared to healthy, UV-protected skin.[29] Furthermore it has been postulated that mesenchymal fibroblast gene signatures are enriched in myCAFs and pro-inflammatory fibroblast gene signatures in iCAFs.[29] It is therefore likely, that the CAFs in cSCC represent the phenotype of reticular dermal fibroblasts, and reflect the invasion of tumor to the deeper reticular layer of the dermis. It has been shown that the expression of PDGFRα by fibroblasts is down-regulated by transforming growth factor-β (TGF-β), suggesting PDGFRα as a marker for non-proliferating fibroblast population.[34,39] In cSCC, both tumor cells and fibroblasts produce TGF-β, and fibroblast-derived TGF-β enhances proteinase expression and promotes invasion of cSCC tumor cells.[40–42] In the progression of ductal breast carcinoma in situ to invasive cancer, the activation of periglandular fibroblasts takes place and is associated with the disruption of basement membrane, downregulation of PDGFRα, and upregulation of PDGFRβ in fibroblasts.[34] In accordance with our findings, high stromal PDGFRα expression has been shown to be associated with more favorable prognosis and high stromal PDGFRβ expression with worse prognosis in non-small cell lung cancer.[43,44]

Our results also show, that a type-II transmembrane serine protease FAP is associated with invasion and metastasis of primary cSCC. Previous studies have shown that expression of FAP by endothelial, immune and malignant epithelial cells is associated with worse prognosis in colorectal, pancreatic, and gastric cancer, and in melanoma.[45] In general, FAP expression in solid tumors is associated with worse prognosis, and FAP overexpression can also be detected in tumor cells.[46] In accordance with our results, FAP expression has been noted in malignant epithelial tumors including cSCC, but not in benign skin tumors.[47]

High expression of POSTN has previously been shown to be associated with poor prognosis in many cancers including cSCC.[16,48,49] Although previous studies have suggested that POSTN is not expressed by cSCC cells,[49] our findings show also epithelial expression of POSTN in a subpopulation of tumors. Furthermore, our results show, that high expression of POSTN both in stromal and epithelial compartments is associated with worse prognosis, in accordance with observations in ovarian and breast cancer.[50,51]

Analysis of multimarker combinations for CAFs identified CAF107 (PDGFRα−/PDGFRβ+/FAP+) as a subset associated with both metastasis and poor prognosis in cSCC. Interestingly, the majority of CAF subsets associated with risk of metastasis or poor prognosis were PDGFRβ and also FAP positive and PDGFRα negative. A four-marker combination in CAF6 (PDGFRβ+/FAP+/PDGFRα−/αSMA−) provided similar metastasis risk and prognosis associations as CAF107, indicating, that the αSMA status had no impact on metastasis risk or prognosis. Based on our results, including analyses with validation cohort, we propose that CAF107 is a potential CAF subset associated with metastasis risk and poor prognosis in primary cSCC. In support for our findings, validation of individual markers of the CAF107 subset in the TCGA data confirmed their prognostic value in lung SCC and HNSCCs.

RDEBSCCs are different from primary UV-cSCCs in terms of etiology, genomic alterations, and clinical behavior.[23,28] Our results demonstrate, that they differ from sporadic UV-cSCCs also with respect to CAFs. RDEBSCCs show low stromal PDGFRβ and Col1 expression in comparison to UV-cSCCs. RDEB is caused by mutations in *COL7A1* gene, which codes for type VII collagen, but it has been shown, that TGF-β signaling plays a role in modulation of disease severity, and that the activated RDEB skin fibroblasts resemble CAFs before the development of SCC.[52,53] RDEB is characterized by chronic ulceration, inflammation and fibrosis of affected skin. The transcriptome of dermal fibroblasts in benign RDEB skin resembles that of UV-cSCC CAFs rather than normal skin fibroblasts, suggesting stromal predisposition of RDEB skin to cSCC development.[54] In addition, in several genodermatoses with cancer risk, including RDEB, the transcriptional profile of dermal fibroblasts is similar and unrelated to corresponding genetic defect.[55] Although the role of PDGFR signaling in the pathogenesis of RDEB is not well known, it has been shown, that PDGFRβ signaling is suppressed in RDEB fibroblasts.[56] Our results provide further evidence, that the CAF phenotype in RDEBSCCs is different from that in UV-cSCCs and that low expression of PDGFRβ in RDEBSCCs is a hallmark of these differences.

Metastasis of primary cSCC results almost exclusively in poor prognosis in patients with cSCC and therefore metastasis risk-associated markers tend to have prognostic power.[3–5] It should be noted, that part of the tissue specimens from normal skin examined in our study were obtained from sun exposed skin and may therefore present certain features of the UV-induced damage of cSCC. In addition, alterations in basement membrane can be detected already in premalignant lesions.[57] It is also of interest, that stromal expression of FAP, αSMA, SPARC, and PDGFRβ was observed in metastases at the same level as in UV-cSCCs, and the POSTN positive fibroblasts were even more frequent in metastases than in primary UV-cSCCs. In addition, the stromal expression of multimarker combinations CAF107 and CAF6 was as strong in metastases as in primary tumors. These observations provide evidence, that the activated CAF phenotype in invasive cSCCs is also present in the stromal compartment of cSCC metastases.

In summary, the results of our study show that alterations in stromal fibroblast activation take place during the progression of cSCC. Early changes in cSCC development include elevation in FAP, αSMA, and SPARC expression, which promotes the development of invasive UV-cSCC. The predominance of CAF107 subset PDGFRα−/PDGFRβ+/FAP+ is associated with invasion and metastasis. In conclusion, we demonstrate that a single CAF marker, PDGFRβ, and especially the CAF subset (CAF107) (PDGFRα−/PDGFRβ+/FAP+) are potential metastasis risk-associated and prognostic biomarkers in cSCC.

AUTHOR CONTRIBUTIONS

Jaakko S. Knuutila: Conceptualization; resources; data curation; formal analysis; validation; investigation; visualization; methodology; writing-original draft; writing-review and editing. **Pilvi Riihilä:** Conceptualization; resources; supervision; writing-original draft; writing-review and editing. **Liisa Nissinen:** Resources; formal analysis;

supervision; validation; investigation; visualization; methodology; writing-original draft; writing-review and editing. **Lauri Heiskanen:** Data curation; formal analysis; validation; visualization; writing-review and editing. **Roosa E. Kallionpää:** Formal analysis; writing-review and editing. **Teijo Pellinen:** Conceptualization; data curation; formal analysis; supervision; validation; investigation; visualization; methodology; writing-original draft; writing-review and editing. **Veli-Matti Kähäri:** Conceptualization; supervision; funding acquisition; writing-original draft; project administration; writing-review and editing. The work reported in the article has been performed by the authors, unless specified in the text.

ACKNOWLEDGEMENTS

We thank Johanna Markola for skillful technical assistance, Annabrita Schoonenberg (FIMM) for performing the mIHC stainings and the staff at the Histology Core of the Institute of Biomedicine at the University of Turku.

FUNDING INFORMATION

The study was supported by Sigrid Jusélius Foundation, Jane and Aatos Erkko Foundation, Finnish Cancer Foundation, Päivikki and Sakari Sohlberg Foundation, Cancer Foundation of the Southwest Finland, Finnish Dermatological Society, The Maud Kuistila Memorial Foundation, Ida Montin Foundation, The Finnish Medical Foundation, and Varsinais-Suomen Sairaanhoitopiiri (project numbers: 11164, 13336). LH is a doctoral candidate in the Doctoral Program for Clinical Investigation of the University of Turku.

CONFLICT OF INTEREST STATEMENT

The authors state no conflict of interest.

DATA AVAILABILITY STATEMENT

Details of the RDEBSCC dataset are provided in the Materials and methods. The other data that support the findings of our study are available from the corresponding author upon reasonable request.

ETHICS STATEMENT

The study was approved by The Ethics Committee of the Hospital District of Southwest Finland (187/2006) and Auria Biobank's Scientific Steering Committee (AB15-9721). The research was carried out according to Declaration of Helsinki and an informed biobank consent was obtained from the patients. Registry study approval for collection and use of clinical and histopathological data was obtained from the Turku University Hospital Clinical Research Centre (TO5/042/18).

ORCID

Jaakko S. Knuutila https://orcid.org/0000-0002-9255-6318
Pilvi Riihilä https://orcid.org/0000-0002-2934-0645
Liisa Nissinen https://orcid.org/0000-0002-6743-6736
Lauri Heiskanen https://orcid.org/0000-0002-0939-5323
Roosa E. Kallionpää https://orcid.org/0000-0003-0146-0060
Teijo Pellinen https://orcid.org/0000-0001-9652-7373
Veli-Matti Kähäri https://orcid.org/0000-0003-2421-9368

TWITTER

Veli-Matti Kähäri *kaharilab*

REFERENCES

1. Venables ZC, Nijsten T, Wong KF, et al. Epidemiology of basal and cutaneous squamous cell carcinoma in the U.K. 2013–15: a cohort study. *Br J Dermatol*. 2019;181:474-482.
2. Venables ZC, Autier P, Nijsten T, et al. Nationwide incidence of metastatic cutaneous squamous cell carcinoma in England. *JAMA Dermatol*. 2019;155:298-306.
3. Burton KA, Ashack KA, Khachemoune A. Cutaneous squamous cell carcinoma: a review of high-risk and metastatic disease. *Am J Clin Dermatol*. 2016;17:491-508.
4. Knuutila JS, Riihilä P, Kurki S, Nissinen L, Kähäri VM. Risk factors and prognosis for metastatic cutaneous squamous cell carcinoma: a cohort study. *Acta Derm Venereol*. 2020;100:adv00266.
5. Schmults CD, Karia PS, Carter JB, Han J, Qureshi AA. Factors predictive of recurrence and death from cutaneous squamous cell carcinoma: a 10-year, single-institution cohort study. *JAMA Dermatol*. 2013;149:541-547.
6. Piipponen M, Riihilä P, Nissinen L, Kähäri VM. The role of p53 in progression of cutaneous squamous cell carcinoma. *Cancer*. 2021;13:4507.
7. Parekh V, Seykora JT. Cutaneous squamous cell carcinoma. *Clin Lab Med*. 2017;37:503-525.
8. Riihilä P, Nissinen L, Knuutila J, Rahmati Nezhad P, Viiklepp K, Kähäri VM. Complement system in cutaneous squamous cell carcinoma. *Int J Mol Sci*. 2019;20:3550.
9. Que SKT, Zwald FO, Schmults CD. Cutaneous squamous cell carcinoma: incidence, risk factors, diagnosis, and staging. *J Am Acad Dermatol*. 2018;78:237-247.
10. Roscher I, Falk RS, Vos L, et al. Validating 4 staging systems for cutaneous squamous cell carcinoma using population-based data: a nested case-control study. *JAMA Dermatol*. 2018;154:428-434.
11. Kalluri R. The biology and function of fibroblasts in cancer. *Nat Rev Cancer*. 2016;16:582-598.
12. Chen Y, McAndrews KM, Kalluri R. Clinical and therapeutic relevance of cancer-associated fibroblasts. *Nat Rev Clin Oncol*. 2021;18:792-804.
13. Van Hove L, Hoste E. Activation of fibroblasts in skin cancer. *J Invest Dermatol*. 2022;142:1026-1031.
14. Chen X, Song E. Turning foes to friends: targeting cancer-associated fibroblasts. *Nat Rev Drug Discov*. 2019;18:99-115.
15. Guweidhi A, Kleeff J, Adwan H, et al. Osteonectin influences growth and invasion of pancreatic cancer cells. *Ann Surg*. 2005;242:224-234.
16. González-González L, Alonso J. Periostin: a matricellular protein with multiple functions in cancer development and progression. *Front Oncol*. 2018;8:225.
17. Nissen NI, Karsdal M, Willumsen N. Collagens and cancer associated fibroblasts in the reactive stroma and its relation to cancer biology. *J Exp Clin Cancer Res*. 2019;38:115.
18. Solé-Boldo L, Raddatz G, Schütz S, et al. Single-cell transcriptomes of the human skin reveal age-related loss of fibroblast priming. *Commun Biol*. 2020;3:188.
19. Reynolds G, Vegh P, Fletcher J, et al. Developmental cell programs are co-opted in inflammatory skin disease. *Science*. 2021;371(6527):eaba6500.
20. Blom S, Paavolainen L, Bychkov D, et al. Systems pathology by multiplexed immunohistochemistry and whole-slide digital image analysis. *Sci Rep*. 2017;7:15580.
21. Viiklepp K, Nissinen L, Ojalill M, et al. C1r upregulates production of matrix metalloproteinase-13 and promotes invasion of cutaneous squamous cell carcinoma. *J Invest Dermatol*. 2022;142:1478-1488.
22. Kivisaari AK, Kallajoki M, Mirtti T, et al. Transformation-specific matrix metalloproteinases (MMP)-7 and MMP-13 are expressed by

tumour cells in epidermolysis bullosa-associated squamous cell carcinomas. *Br J Dermatol*. 2008;158:778-785.
23. Cho RJ, Alexandrov LB, den Breems NY, et al. APOBEC mutation drives early-onset squamous cell carcinomas in recessive dystrophic epidermolysis bullosa. *Sci Transl Med*. 2018;10:eaas9668.
24. Berg S, Kutra D, Kroeger T, et al. Ilastik: interactive machine learning for (bio)image analysis. *Nat Methods*. 2019;16:1226-1232.
25. Stirling DR, Swain-Bowden MJ, Lucas AM, Carpenter AE, Cimini BA, Gooodman A. CellProfiler 4: improvements in speed, utility and usability. *BMC Bioinformatics*. 2021;22:433.
26. Cancer Genome Atlas Research Network, Weinstein JN, Collisson EA, et al. The Cancer Genome Atlas Pan-cancer analysis project. *Nat Genet*. 2013;45:1113-1120.
27. Uhlen M, Zhang C, Lee S, et al. A pathology atlas of the human cancer transcriptome. *Science*. 2017;357:eaan2507.
28. Tartaglia G, Cao Q, Padron ZM, South AP. Impaired wound healing, fibrosis, and cancer: the paradigm of recessive dystrophic epidermolysis bullosa. *Int J Mol Sci*. 2021;22:5104.
29. Schütz S, Solé-Boldo L, Lucena-Porcel C, et al. Functionally distinct cancer-associated fibroblast subpopulations establish a tumor promoting environment in squamous cell carcinoma. *Nat Commun*. 2023;14:5413.
30. Karnoub AE, Dash AB, Vo AP, et al. Mesenchymal stem cells within tumour stroma promote breast cancer metastasis. *Nature*. 2007;449:557-563.
31. Shinagawa K, Kitadai Y, Tanaka M, et al. Stroma-directed imatinib therapy impairs the tumor-promoting effect of bone marrow-derived mesenchymal stem cells in an orthotopic transplantation model of colon cancer. *Int J Cancer*. 2013;132:813-823.
32. Kitadai Y, Sasaki T, Kuwai T, et al. Expression of activated platelet-derived growth factor receptor in stromal cells of human colon carcinomas is associated with metastatic potential. *Int J Cancer*. 2006;119:2567-2574.
33. Östman A. PDGF receptors in tumor stroma: biological effects and associations with prognosis and response to treatment. *Adv Drug Deliv Rev*. 2017;121:117-123.
34. Paulsson J, Sjöblom T, Micke P, et al. Prognostic significance of stromal platelet-derived growth factor β-receptor expression in human breast cancer. *Am J Pathol*. 2009;175:334-341.
35. Hägglöf C, Hammarsten P, Josefsson A, et al. Stromal PDGFRβ expression in prostate tumors and non-malignant prostate tissue predicts prostate cancer survival. *PLoS One*. 2010;5:e10747.
36. Frings O, Augsten M, Tobin NP, et al. Sonnhammer ELL prognostic significance in breast cancer of a gene signature capturing stromal PDGF signaling. *Am J Pathol*. 2013;182:2037-2047.
37. Sasaki K, Sugai T, Ishida K, et al. Analysis of cancer-associated fibroblasts and the epithelial-mesenchymal transition in cutaneous basal cell carcinoma, squamous cell carcinoma, and malignant melanoma. *Hum Pathol*. 2018;79:1-8.
38. Philippeos C, Telerman SB, Oulès B, et al. Spatial and single-cell transcriptional profiling identifies functionally distinct human dermal fibroblast subpopulations. *J Invest Dermatol*. 2018;138:811-825.
39. Crowley MR, Bowtell D, Serra R. TGF-β, c-Cbl, and PDGFR-α the in mammary stroma. *Dev Biol*. 2005;279:58-72.
40. Leivonen SK, Ala-aho R, Koli K, Grénman R, Peltonen J, Kähäri VM. Activation of Smad signaling enhances collagenase-3 (MMP-13) expression and invasion of head and neck squamous carcinoma cells. *Oncogene*. 2006;25:2588-2600.
41. Siljamäki E, Rappu P, Riihilä P, Nissinen L, Kähäri VM, Heino J. H-Ras activation and fibroblast-induced TGF-β signaling promote laminin-332 accumulation and invasion in cutaneous squamous cell carcinoma. *Matrix Biol*. 2020;87:26-47.
42. Siljamäki E, Riihilä P, Suwal U, et al. Inhibition of TGF-β signaling, invasion and growth of cutaneous squamous cell carcinoma by PLX8394. *Oncogene*. 2023;42:3633-3647.
43. Kilvaer TK, Rakaee M, Hellevik T, et al. Differential prognostic impact of platelet-derived growth factor receptor expression in NSCLC. *Sci Rep*. 2019;9:10163.
44. Pellinen T, Paavolainen L, Martín-Bernabé A, et al. Fibroblast subsets in non-small cell lung cancer: associations with survival, mutations, and immune features. *J Natl Cancer Inst*. 2023;115:71-82.
45. Fitzgerald AA, Weiner LM. The role of fibroblast activation protein in health and malignancy. *Cancer Metastasis Rev*. 2020;39:783-803.
46. Liu F, Qi L, Liu B, et al. Fibroblast activation protein overexpression and clinical implications in solid tumors: a meta-analysis. *PLoS One*. 2015;10:e0116683.
47. El Khoury J, Kurban M, Kibbi AG, Abbas O. Fibroblast-activation protein: valuable marker of cutaneous epithelial malignancy. *Arch Dermatol Res*. 2014;306:359-365.
48. Xu X, Chang W, Yuan J, et al. Periostin expression in intratumoral stromal cells is prognostic and predictive for colorectal carcinoma via creating a cancer-supportive niche. *Oncotarget*. 2016;7:798-813.
49. Lincoln V, Chao L, Woodley DT, et al. Overexpression of stromal periostin correlates with poor prognosis of cutaneous squamous cell carcinomas. *Exp Dermatol*. 2021;30:698-704.
50. Sung PL, Jan YH, Lin SC, et al. Periostin in tumor microenvironment is associated with poor prognosis and platinum resistance in epithelial ovarian carcinoma. *Oncotarget*. 2016;7:4036-4047.
51. Kim GE, Lee JS, Park MH, Yoon JH. Epithelial periostin expression is correlated with poor survival in patients with invasive breast carcinoma. *PLoS One*. 2017;12:e0187635.
52. Odorisio T, Di Salvio M, Orecchia A, et al. Monozygotic twins discordant for recessive dystrophic epidermolysis bullosa phenotype highlight the role of TGF-β signalling in modifying disease severity. *Hum Mol Genet*. 2014;23:3907-3922.
53. Condorelli AG, Dellambra E, Logli E, Zambruno G, Castiglia D. Epidermolysis bullosa-associated squamous cell carcinoma: from pathogenesis to therapeutic perspectives. *Int J Mol Sci*. 2019;20:5707.
54. Ng YZ, Pourreyron C, Salas-Alanis JC, et al. Fibroblast-derived dermal matrix drives development of aggressive cutaneous squamous cell carcinoma in patients with recessive dystrophic epidermolysis bullosa. *Cancer Res*. 2012;72:3522-3534.
55. Chacón-Solano E, León C, Díaz F, et al. Fibroblast activation and abnormal extracellular matrix remodelling as common hallmarks in three cancer-prone genodermatoses. *Br J Dermatol*. 2019;181:512-522.
56. Martínez-Martínez E, Tölle R, Donauer J, Gretzmeier C, Bruckner-Tuderman L, Dengjel J. Increased abundance of Cbl E3 ligases alters PDGFR signaling in recessive dystrophic epidermolysis bullosa. *Matrix Biol*. 2021;103-104:58-73.
57. Karppinen SM, Honkanen HK, Heljasvaara R, et al. Collagens XV and XVIII show different expression and localisation in cutaneous squamous cell carcinoma: type XV appears in tumor stroma while XVIII becomes upregulated in tumor cells and lost from microvessels. *Exp Dermatol*. 2016;25:348-354.

SUPPORTING INFORMATION

Additional supporting information can be found online in the Supporting Information section at the end of this article.

How to cite this article: Knuutila JS, Riihilä P, Nissinen L, et al. Cancer-associated fibroblast activation predicts progression, metastasis, and prognosis of cutaneous squamous cell carcinoma. *Int J Cancer*. 2024;1-16. doi:10.1002/ijc.34957